



Embedded Multi-Tone Ultrasonic Excitation and Continuous-Scanning Laser Doppler Vibrometry for Rapid and Remote Imaging of Structural Defects

Eric B. Flynn

► To cite this version:

Eric B. Flynn. Embedded Multi-Tone Ultrasonic Excitation and Continuous-Scanning Laser Doppler Vibrometry for Rapid and Remote Imaging of Structural Defects. EWSHM - 7th European Workshop on Structural Health Monitoring, IFFSTTAR, Inria, Université de Nantes, Jul 2014, Nantes, France. hal-01021054

HAL Id: hal-01021054

<https://inria.hal.science/hal-01021054>

Submitted on 9 Jul 2014

HAL is a multi-disciplinary open access archive for the deposit and dissemination of scientific research documents, whether they are published or not. The documents may come from teaching and research institutions in France or abroad, or from public or private research centers.

L'archive ouverte pluridisciplinaire **HAL**, est destinée au dépôt et à la diffusion de documents scientifiques de niveau recherche, publiés ou non, émanant des établissements d'enseignement et de recherche français ou étrangers, des laboratoires publics ou privés.

EMBEDDED MULTI-TONE ULTRASONIC EXCITATION AND CONTINUOUS-SCANNING LASER DOPPLER VIBROMETRY FOR RAPID AND REMOTE IMAGING OF STRUCTURAL DEFECTS

Eric B. Flynn¹

¹ *Los Alamos National Laboratory, PO Box 1663 MS-T001, Los Alamos, NM, 87501,
eflynn@lanl.gov*

ABSTRACT

We describe a novel method for rapidly measuring local wave dispersion properties using steady-state excitation continuous-scanning laser Doppler vibrometry (CSLDV). In our approach, we excite a structure with a periodic ultrasonic waveform constructed from the sum of several single-tone waveforms. The structure is excited continuously, bringing it to steady-state. We then measure the steady-state response of the structure through CLSDV. The continuous scan gives a one-dimensional time-history of measured response velocity, which we convert to time histories of the instantaneous amplitude and phase for each excitation frequency component. We then map these instantaneous amplitudes and phases to a discretized grid of points spanning the scan area. Finally, through wavenumber processing, we convert these 2D maps into local estimates of wavenumber. Since this is done for each excitation frequency, we are left with a set of frequency samples of local frequency-wavenumber dispersion curves at each spatial sample point in the structure. Since defects alter local dispersion properties in a predictable way, these dispersion curve maps offer an effective means of both locating and characterizing defects such as corrosion and delamination.

KEYWORDS : *Ultrasonic Guided Waves, Scanning Laser Doppler Vibrometry*

INTRODUCTION

Scanning ultrasound systems are commonly used for nondestructive evaluation, but not for structural health monitoring. This is because ultrasonic scanning systems are too slow and disruptive to be of practical use when the inspected structure is in operation. For contact or air-coupled actuation and sensing, a scanning apparatus must be installed so that the transducers can physically reach all of the inspection points. For nearly all scanning ultrasound systems, including remote laser-based systems, the scan speed is limited by the time it takes at each inspection point to excite a pulse, measure the response, and wait for the wave-reverberations to die out [1,2]. At a minimum, this takes approximately 5 ms per scan point. For a one megapixel scan, that equates to a scan time of well over one hour. That is a long time for an operational structure to “hold still”.

Embedded ultrasonic guided wave systems hold a lot of potential [3,4], but still suffer from low data density compared to scanning systems. With a relatively small, fixed set of inspection points, i.e. transducer locations, we are oftentimes faced with having insufficient measurement data to separate damage from normal operational variability, or to clearly characterize the size, type, and/or shape of the damage.

We previously demonstrated a new technique for generating full field ultrasonic scan images using single-tone excitation [5]. With a steady, single tone excitation, the structure is brought to a steady-state response. This eliminates the need to wait for a transient response at each scan point, increasing the maximum scan speeds by one or two orders of magnitude. From the measured response, estimates of local wavenumber are extracted to form damage-revealing maps.

So far, this approach has been limited to the measurement of the response at a single tone. In this paper, we introduce a means of expanding this approach to multiple tones without sacrificing scan speed. Ultimately, our goal is to be able to simultaneously estimate multiple structural parameters, such as modulus, thickness, and density, using a single steady-state scan.

1 MATERIALS AND METHODS

1.1 Measurement Approach

The measurement system consists of (1) a set of embedded transducers for ultrasonic excitation, (2) and signal generator for driving the transducers, (3) a laser Doppler vibrometer for measuring the response, (4) a pair of galvanometer mirrors for steering the LDV, and (5) a laptop computer for control and data acquisition.

First, the structure is excited with a periodic signal consisting of N ultrasonic tones with frequencies $f_1 \dots f_N$. These tones are excited continuously during the entire measurement process, and without windowing. This brings the structure to a steady-state response that, in turn, is a superposition of the excitation tones, presuming the structure response is predominantly linear-elastic.

Next, a Polytech LDV is swept continuously over a predefined region of the structure using a pair of Thorlabs galvanometric mirrors at a rate s . As the laser moves back and forth over the scan region, a National Instruments DAQ PXI card and laptop computer record the one-dimensional stream of voltage values from the LDV at a rate of one million samples per second. These voltages correspond to measured velocities along the axis of the beam according to the LDV system sensitivity.

1.2 Signal Processing Approach

In software, as the voltage values stream in, they are broken into M equally sized blocks, $v_1 \dots v_M$, each of which corresponds to a small, 1-5 mm segment of the scan path. The discrete Fourier transform is computed for each segment and at each of the individual excitation tones according to

$$r'_m[f_i] = \sum_t v_m[t] \exp(-j2\pi f_i t) \quad (1)$$

These N complex values, $r'_m[f_1 \dots f_N]$, represent the steady-state responses to each tone of each local segment of the scan path as the laser moved across it. In order to obtain a full field response, we need to “lock” all of the local responses to the same phase. To do this, we will use the first scan segment as the reference, and phase shift all of the subsequent segments by the time it took the LDV to reach that point. If each block corresponds to a path segment of length L , then we phase shift each segment according to

$$r_m[f_i] = r'_m[f_i] \exp(-j2\pi f_i \phi_m) \quad (2)$$

where $\phi_m = mL/s$. The N phase-locked complex response values for each signal block are then mapped back to the center points of the corresponding scan path segments in order to form N two-dimensional grids, which represent the maps of complex steady state responses at each of the excitation tones. We treat this set of two-dimensional grids as a single three-dimensional matrix with elements indexed according to two spatial coordinates and a frequency value, or $r[x, y, f]$.

The final step is transform each response map into a map of local wavenumber estimates. We do this by first passing the map through a bank of narrowband wavenumber filters. We then compute the two-dimensional envelope of each filter response. Finally, we choose as the wavenumber estimate for each map grid point the center-wavenumber whose corresponding filter maximized the wavenumber at that point. A more detailed description of this procedure can be found in [5] and [2]. This gives us a wavenumber estimate for each excitation tone and for each spatial coordinate in the scan region, or $w[x, y, f]$. Alternatively, this can be thought of as samples of a frequency-wavenumber dispersion curve at each scan pixel.

1.3 Test Descriptions

We considered two simple structures for testing the approach. The first sample was a 320 mm square section of a 1.5 mm thick aluminum panel with a 10 mm long oblong-shaped corrosion mark on the hidden surface. A photograph of the corrosion mark is shown in Figure 1. The second sample was a 300 mm by 7 mm thick square carbon fiber reinforced polymer (CFRP) panel with a hidden projectile impact delamination.

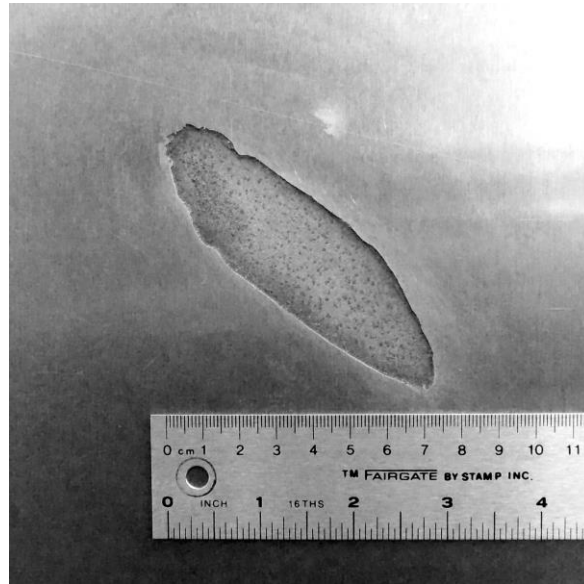


Figure 1: Photograph of corrosion mark on hidden surface of aluminum panel

The two structures were excited with a pair of matching sandwich transducers. These transducers, which are used for ultrasonic cleaning applications, are designed to be effective at particular frequencies. Using an impedance analyzer, we determined that these transducers operated most effectively at 36.92 kHz, 65.04 kHz, and 80.40 kHz. As such, these frequencies were chosen as the composing frequencies of the multi-tone excitation signal. Figure 2 shows a snapshot of the resulting multi-tone signal. The drive signal was amplified to a peak voltage of 80 volts. The structure was discretized to 2 mm intervals and scanned at a linear rate of 16 m/s (or 115 square meters per hour) from a distance of 3 meters.

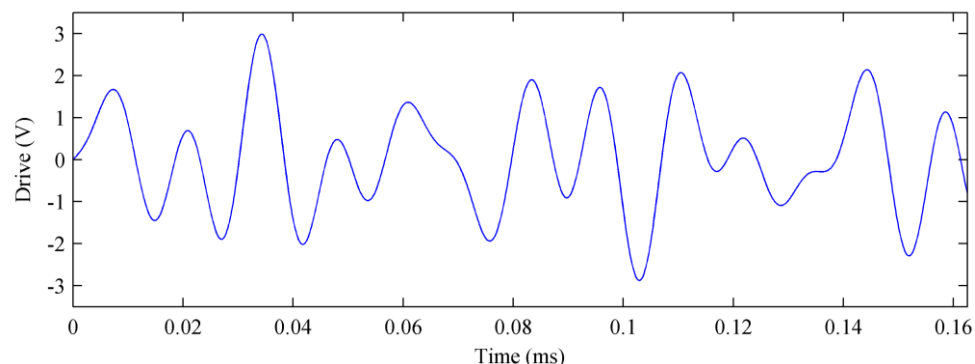


Figure 2 : Multi-tone excitation signal composed of frequencies 37 kHz, 65 kHz, and 80 kHz

2 RESULTS

2.1 Aluminum Panel

Figure 3 shows the combined steady-state response measurement for the aluminum sample. Figure 4 shows the response of the aluminum panel broken apart according to each of the three excitation tones. In reality, the responses to the three individual tones are computed first according to (1) and then summed together to form the combined response measurement. Note that the subtle change in the wave pattern due to the corrosion is not easily distinguished by simply looking at the response images.

Figure 5 shows the resulting local wavenumber estimate maps for each of the three excitation tones. The results indicate that the presence of the corrosion resulted in a 10-20% increase in local wavenumber. Keep in mind that all three maps were generated from a single scan. To help quantify the accuracy of the wavenumber estimation process, we calculated summary statistics of the “heathy” northwest quadrant of the wavenumber map as well as the theoretical dispersion curve for the 1.5 mm aluminum plate [6]. In Figure 6 we show the mean, minimum and maximum of the wavenumber estimates plotted against the corresponding tone frequencies and on top of the theoretical dispersion curve. This plot also shows the peak wavenumber in the corrosion region. The estimated wavenumbers show good agreement with the theoretical values in the aluminum plate.

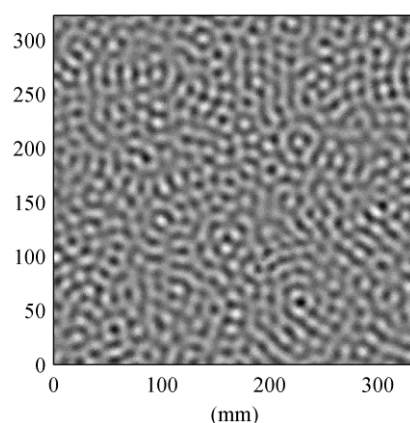


Figure 3 : Combined measured steady-state response in 1.5 mm thick corroded aluminum panel to excitation consisting of combined 37 kHz, 65 kHz, and 80 kHz tones.

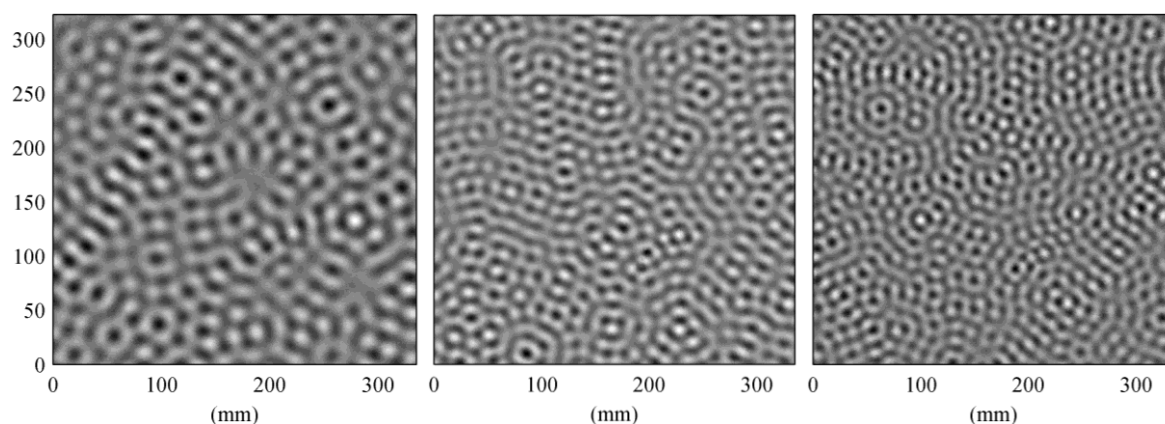


Figure 4: Individual single-tone measured steady-state responses in 1.5 mm thick corroded aluminum panel to excitation consisting of combined 37 kHz, 65 kHz, and 80 kHz tones, shown left to right.

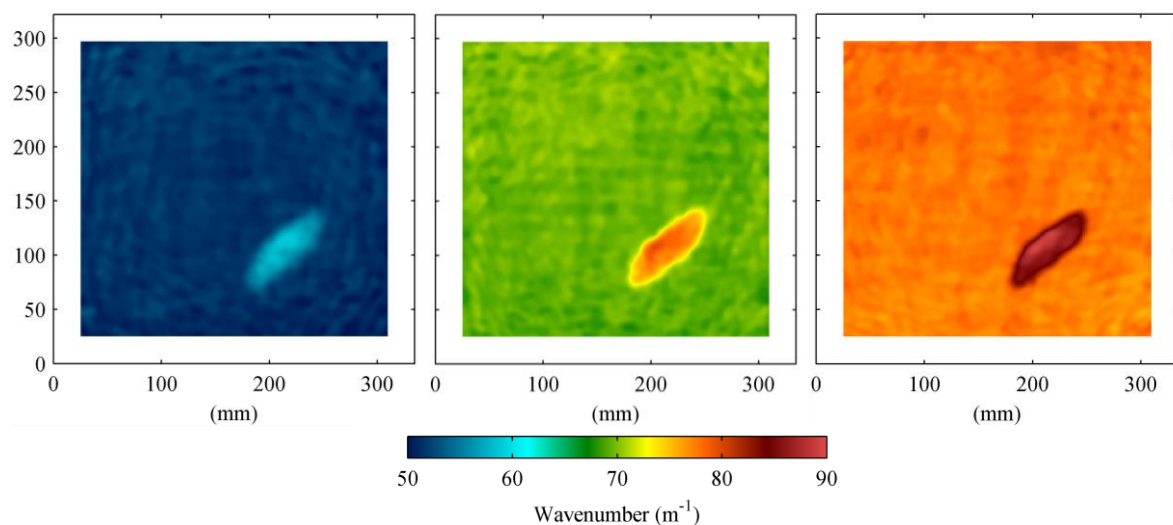


Figure 5: Maps of local wavenumber estimates for 37 kHz, 65 kHz, and 80 kHz response frequencies, shown left to right, for a 1.5 mm thick corroded aluminum panel

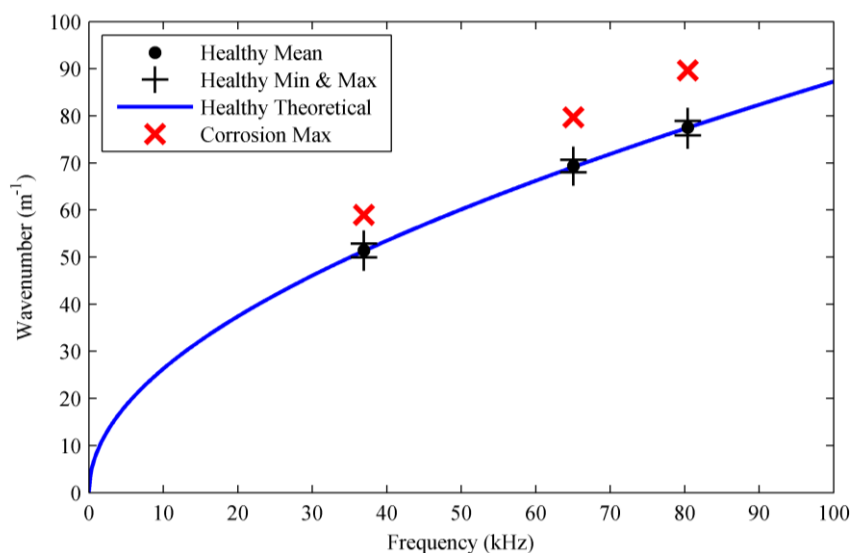


Figure 6: Dispersion curve sample estimates with theoretical dispersion curve for 1.5 mm thick aluminum panel. Shown are samples from both the healthy and corroded regions of the panel.

2.2 Composite Panel

Figure 7 and Figure 8 show the combined response measurement and the response measurements divided according to each excitation tone. In the composite sample, the change in wavenumber is evident by just looking at the raw responses. Figure 9 shows the resulting local wavenumber estimate maps. Effective reductions in material thickness leads to an increase in local wavenumber. Therefore, in a composite specimen, a higher wavenumber corresponds to the delamination occurring closer to the scan surface. The effect on imaging resolution is evident in these images, with the symmetric, two-lobe delamination pattern becoming clearer with increasing excitation frequency.

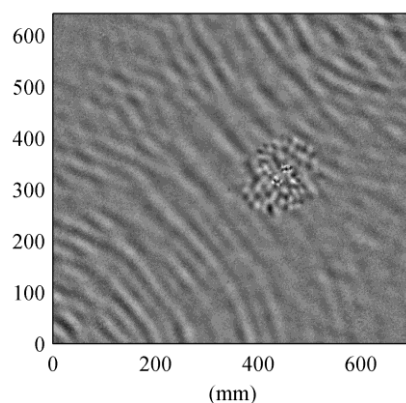


Figure 7 : Combined measured steady-state response in 1.5 mm thick corroded aluminum panel (left) and CFRP panel (right) to excitation consisting of combined 37 kHz, 65 kHz, and 80 kHz tones.

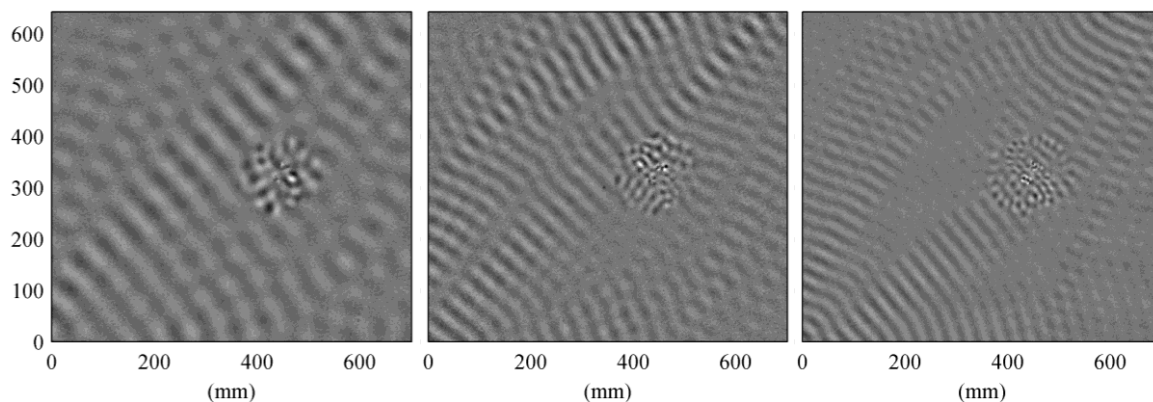


Figure 8: Individual single-tone measured steady-state responses in impacted CFRP panel to excitation consisting of combined 37 kHz, 65 kHz, and 80 kHz tones, shown left to right.

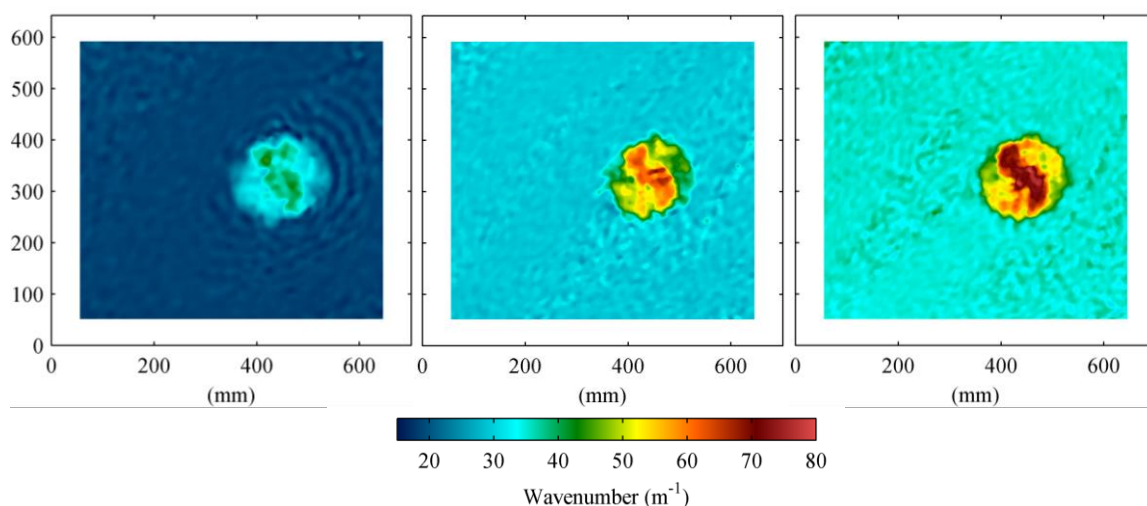


Figure 9: Maps of local A_0 wavenumber estimates for 37 kHz, 65 kHz, and 80 kHz response frequencies, shown left to right, for impacted CFRP panel.

3 DISCUSSION

The results show that, with proper synchronization and isolation of each of frequency tone, it is possible to extract multiple samples of a frequency-wavenumber dispersion curve using a single steady-state response scan. However, the use of multiple excitation tones comes with an inherent tradeoff. More information can be extracted with more frequencies, but at the cost of less per-tone excitation energy. The choice of tone count will therefore be application-dependent. For effective multiple-parameter characterization, we suspect that the ability to estimate wavenumber at multiple tones will be important. Following a more quantitative analysis of accuracy and resolution, the next step will be to derive estimators that can translate the multiple wavenumber estimates into physical quantities such as plate thickness or delamination depth.

REFERENCES

- [1] Dhital D, Lee JR, Park CY, Flynn E. Laser excitation and fully non-contact sensing ultrasonic propagation imaging system for damage evaluation. International Society for Optics and Photonics; 2012. p. 83430D–83430D.
- [2] Flynn EB, Chong SY, Jarmer GJ, Lee J-R. Structural imaging through local wavenumber estimation of guided waves. NDT E Int. 2013 Oct;59:1–10.
- [3] Croxford A, Wilcox P, Drinkwater B, Konstantinidis G. Strategies for guided-wave structural health monitoring. Proc. R. Soc. Math. Phys. Eng. Sci. 2007;463(2087):2961.
- [4] Flynn EB, Todd MD, Wilcox PD, Drinkwater BW, Croxford AJ. Maximum-likelihood estimation of damage location in guided-wave structural health monitoring. Proc. R. Soc. Math. Phys. Eng. Sci. 2011;467(2133):2575–2596.
- [5] Flynn EB, Jarmer GJ. High-Speed, Non-Contact, Baseline-Free Imaging of Hidden Defects Using Scanning Laser Measurements of Steady-State Ultrasonic Vibration. In: Structural Health Monitoring 2013. Stanford, CA: DEStech Publications, Inc.; 2013. p. 1186–1193.
- [6] Rose J. Ultrasonic waves in solid media. Cambridge; New York: Cambridge University Press; 2004.